

In-Orbit Relative Amplitude and Phase Antenna Pattern Calibration for Tandem-L

Gerhard Krieger, Sigurd Huber, Marwan Younis, Alberto Moreira, Jens Reimann, Patrick Klenk, Manfred Zink, Michelangelo Villano, Felipe Queiroz de Almeida

Microwaves and Radar Institute, German Aerospace Center (DLR), Germany

Abstract

Precise knowledge of the far-field antenna patterns associated with individual receive channels of a multi-channel SAR system is of fundamental importance to operate the radar instrument in advanced imaging modes. A prominent example is Tandem-L which uses a large deployable parabolic reflector that is illuminated by a digital feed array with multiple receive channels. This architecture enables, in combination with an appropriate on-board signal processing, the acquisition of a wide image swath by simultaneously recording multiple scattered radar echoes with a set of narrow elevation beams that are steered in real time towards the angles of the arriving wavefronts. As such a multiple elevation beam technique is prone to range ambiguities, optimized real-time beamformers are considered that maximize their gain in the direction of the desired radar echo and suppress, at the same time, the range ambiguous radar echoes arriving from different angles. The implementation of these advanced real-time beamforming techniques requires, however, precise knowledge of the amplitude and phase of the secondary far-field antenna patterns associated with the excitation of single feed elements. As it is impossible to measure these complex antenna patterns on ground with sufficient accuracy, we propose here a novel technique that enables a highly accurate in-orbit measurement of the relative amplitude and phase of the far-field secondary antenna patterns associated with individual feed elements. The key idea is to collect SAR data in space by a set of dedicated calibration flights, where the signals from all feed elements are simultaneously recorded in a transparency mode, i.e., without any real-time beamforming on board the satellite. The multichannel data are then transferred to the ground, where the relative antenna pattern information is extracted and calibrated beamforming coefficients are derived, as required for the implementation of advanced SAR modes. This paper provides an overview of the proposed multichannel antenna calibration technique and demonstrates the superior SAR imaging performance that can be achieved by employing this technique in conjunction with a series of especially designed calibration flights over natural terrain with known topography.

1 Introduction

Tandem-L is a proposal for a highly innovative SAR mission to monitor the Earth system with unprecedented spatial and temporal resolution [1]. To meet the demanding mission requirements, a new SAR instrument architecture and imaging mode has been developed [2], [3]. The system architecture is based on a large parabolic reflector antenna that is illuminated by a digital feed with multiple elevation channels (cf. Figure 1) [4]. As each feed element is associated with a different secondary beam, it becomes possible to image a wide swath with high Rx gain by a time-variant combination of the feed signals in synchrony with the expected direction of arrival of the desired radar echo [5], [6]. The imaging capacity is further increased by using not only one but multiple elevation beams that map multiple swaths at the same time [7]. As these swaths are separated by blind ranges, several strategies and modes have been proposed to avoid such gaps in the SAR image [8]. Out of these modes, Tandem-L will employ a technique where the pulse repetition interval is rapidly changed from pulse to pulse [9]. This technique, now denoted as staggered SAR, has been further analyzed and elaborated in detail in [10], [11]. In combination with an optimized Tandem-L reflector and feed system it becomes

then possible to map a 350 km wide swath with an azimuth resolution of 7 m, thereby significantly improving the imaging capacity if compared to state-of-the-art L-band SAR systems like ALOS-2 or even the C-band satellite constellation Sentinel-1A and 1B.

While staggered SAR enables the acquisition of an ultra-wide image swath with high resolution, it requires also a notable oversampling in azimuth. Such an increase of the average pulse repetition frequency (PRF) is mandatory to avoid a rise of azimuth ambiguities caused by missing samples along the synthetic aperture [12]. The high PRF will, however, also increase the susceptibility to range ambiguities. Range ambiguity suppression is further challenged by the required wide swath illumination, which causes multiple mutually ambiguous radar echoes to arrive at the same time from different elevation angles but with comparable magnitudes (cf. Figure 1). This poses high demands on the multichannel receiver system which has to steer multiple elevation beams in real time towards the radar echoes' expected directions of arrival. The shape of each of these receiver beams must be adjusted to maximize for each instant of time the antenna gain in the direction of the desired radar echo, while minimizing the gain towards the arrival angles of the interfering range ambiguous radar echoes.

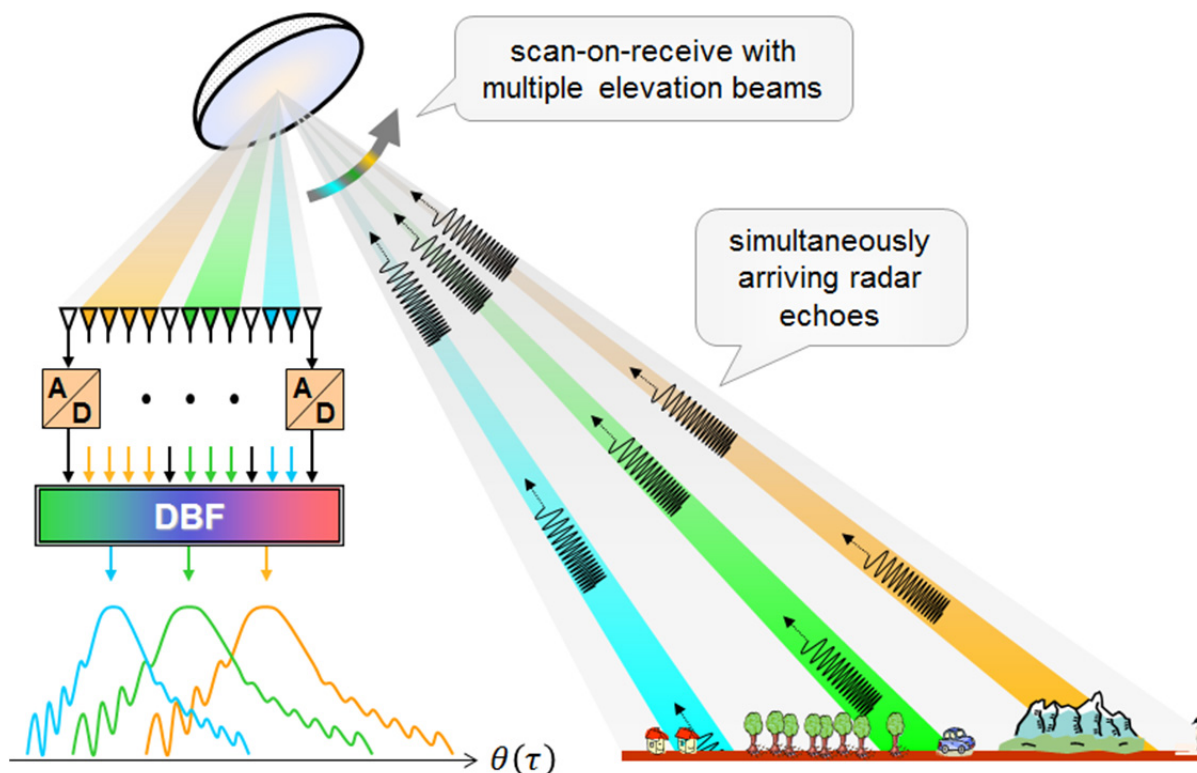


Figure 1: Reflector SAR with multiple elevation beams. Digital beamforming on receive plays a crucial role for the reliable separation of the simultaneously arriving radar echoes from range-ambiguous positions.

Several beamforming algorithms have been developed to address this challenge, but their performance depends crucially on the accurate knowledge of the amplitude and phase of the secondary beam patterns associated with individual feed array elements [4], [13]. While this knowledge is less important for a planar array, where the element patterns are typically pretty similar and the overall radiation performance is primarily determined by the array's geometry and excitation, it becomes mandatory for reflector SAR systems, where each feed has its own element pattern that points its secondary beam to a different direction. As it is impossible to measure the antenna patterns for a SAR system like Tandem-L with sufficient accuracy before launch on the ground, one needs an alternative strategy to obtain the required far-field pattern information. One established approach is the use of dedicated calibration targets like corner reflectors or transponders [14], [15]. A very large number of calibration targets would, however, be required to meet the accuracy requirements as the antenna patterns associated with individual feed elements cover different areas and are moreover characterized by a high degree of spatial variation, which is further complicated by the fact that the patterns are typically non-separable in elevation and azimuth. Another approach, which was successfully applied for TerraSAR-X [16], is based on the use of an appropriate antenna model, but the requirements regarding the precise knowledge of the deployed reflector's attitude and shape are rather high to meet the demanding performance requirements [17].

2 In-Orbit Multichannel Antenna Pattern Calibration

As a complement to the conventional antenna pattern estimation and modeling techniques discussed before, we propose here a new multichannel calibration approach that enables highly accurate in-orbit measurements of the amplitude and phase differences between the secondary far-field patterns of the feed elements/channels. The proposed technique is capable of providing this information in two dimensions without the need of dedicated calibration targets and/or a sophisticated antenna model. The core concept is to operate the SAR system over an appropriately chosen natural scene with known topography in a series of dedicated calibration modes, which are described in more detail in the following subsections. The basic idea of this technique has already been suggested in the context of the cross-elevation beam range ambiguity suppression technique CEBRAS [18], and is here further elaborated in view of the demanding requirements for Tandem-L.

2.1 Low PRF Antenna Calibration (LPAC)

As a first calibration mode, we consider an operation with a very low pulse repetition frequency (PRF), so that only a single radar echo arrives at the radar satellite at any time. A wide swath is illuminated, and all elevation channels simultaneously record and digitize their received signals independently from each other without applying any on-board beamforming. As the total data

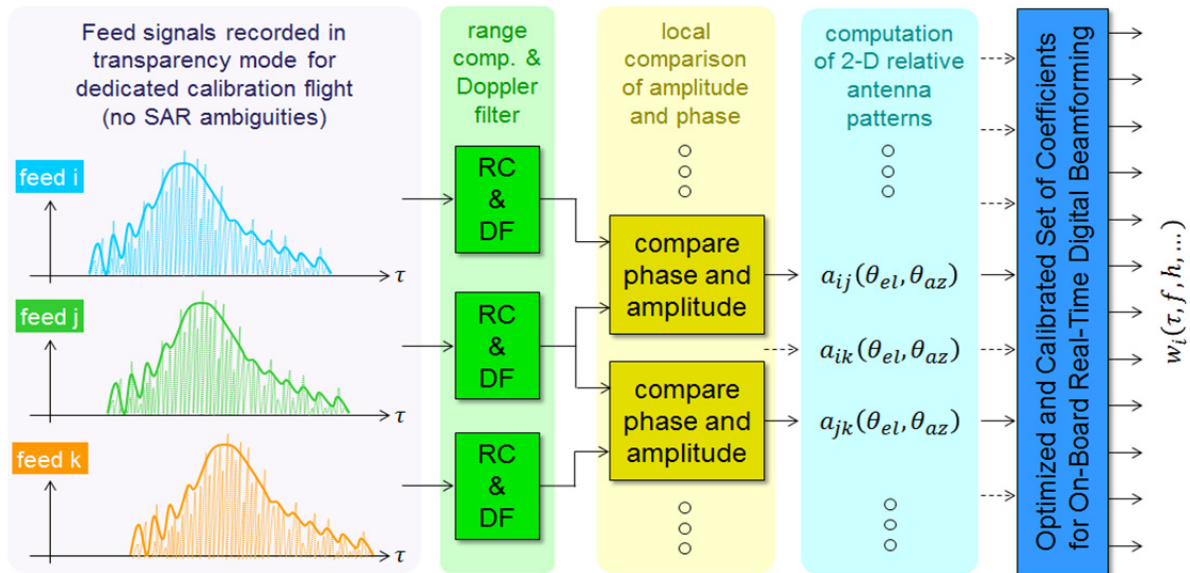


Figure 2: Illustration of the basic steps of the proposed multichannel antenna calibration. The recorded radar data of each feed are first individually range compressed (RC) and bandpass-filtered in the Doppler domain (DF). In a second step, the feed signals are mutually compared and relative amplitude and phase patterns are computed as a function of range and Doppler. In a third step, the relative amplitude and phase patterns are transformed from the range-Doppler coordinates to the corresponding elevation and azimuth angles. This transformation requires knowledge of the satellite's orbit and attitude in combination with an appropriate digital elevation model. Finally, the relative pattern information is used to calculate a calibrated and optimized set of digital beamforming coefficients that are uploaded to the satellite.

rate of this transparency mode is likely to exceed the capacity of the input channel to the on-board memory, it is suggested to reduce the RF bandwidth in this mode. Tandem-L is, for example, capable to handle in its nominal staggered SAR mode the radar signals from five elevation beams, each recording a radar echo with an RF bandwidth of 84 MHz. A reduction to, e.g., 10 MHz allows therefore the simultaneous recording of all 35 feed signals without increasing the internal data rate.¹ If necessary, the full bandwidth can then be covered by subsequent measurements where the range center frequency is appropriately varied from data take to data take. The multichannel radar data acquired in this dedicated antenna calibration mode are then transmitted to the ground, where they are further evaluated.

The evaluation starts with a range compression of the signals from the individual elevation channels. Assuming a calibration scene that is sufficiently flat and free of layover, there exists thereafter a one-to-one relation between the instant of time in the range-compressed data and the elevation angle from which the radar echoes are arriving. This relationship is easily derived from the imaging geometry and the known topography of the calibration scene.² However, as the low PRF of the LPAC mode does not allow for azimuth focusing, radar echoes arriving at the same time from multiple azimuth angles cannot be separated from each other. A compari-

son of the recorded feed signals in amplitude and phase yields therefore an estimate of the relative antenna patterns integrated over azimuth.³ The performance simulations in Section 3 reveal that this information is nevertheless well suited to derive beamforming coefficients for highly efficient range ambiguity suppression without detailed a priori pattern knowledge.

2.2 High PRF Antenna Calibration (HPAC)

While the LPAC mode outlined in the previous section is well suited to derive appropriate weights for elevation beamforming, a more detailed knowledge of the relative azimuth antenna patterns may be of interest to further improve the SAR imaging performance and to support the end-to-end system calibration.

For this, we suggest to acquire SAR data over an appropriate scene in the high PRF antenna calibration (HPAC) mode. In contrast to the LPAC mode, only a narrow swath is illuminated by transmitting with one or a small subset of the available feed elements. The reduced swath illumination provides an efficient means to suppress range ambiguities as they are, in contrast to the nominal wide-swath staggered SAR mode, already suppressed by the Tx pattern.⁴ The calibration data for the full swath extension can then be recovered by combining the data from a series of measurements where different subswaths are illuminated.⁵ In comparison to the

¹ The reduced RF bandwidth is also beneficial to increase the SNR of each recorded signal. By this, even the weak echoes from the antenna sidelobes can be acquired with sufficient accuracy. The SNR could be further improved by increasing the length of each individual pulse, if compared to the rather short pulses used in the staggered SAR mode.

² A coarse DEM with a resolution in the order of 100 m is considered as sufficient.

³ The involved azimuth angles are typically small and span for Tandem-L an angular interval in the order of 1°.

⁴ Residual range ambiguities could, in principle, also be resolved by blind source separation as proposed in [18].

⁵ For stability reasons, these measurements can be combined into a single data take, where the Tx pattern sequence is similar to that of a ScanSAR mode.

staggered SAR mode, the use of a constant PRF avoids, moreover, the loss of azimuth samples and enables therefore an excellent suppression of the azimuth ambiguities. Stated differently, a reduced PRF could be used to achieve the same azimuth ambiguity-to-signal ratio.

The HPAC data are then transmitted to the ground and further analyzed as illustrated in Figure 2. The evaluation starts again with a range compression of each individual feed signal. In contrast to the LPAC mode, the range-compressed data are then transformed to the range-Doppler domain (or decomposed into multiple azimuth looks) which provides the basis for a two-dimensional analysis of the antenna patterns [18]. In the next step, the phases and amplitudes from different feed elements are compared in a local neighborhood of each range-Doppler bin. This comparison may either be based on local averages, or on a more elaborated model-based evaluation. A pretty simple approach could, for example, start from the hypothesis that the signals from different feed elements $u_i(\tau, f_D)$ and $u_j(\tau, f_D)$ are, for each range-Doppler bin (τ, f_D) , scaled functions of the same backscatter, i.e., they are related by complex weights $a_{ji}(\tau, f_D)$. Each feed signal will also be subject to mutually independent noise $n(\tau, f_D)$ and we obtain

$$\begin{aligned} u_i(\tau, f_D) &= u(\tau, f_D) + n_i(\tau, f_D) \\ u_j(\tau, f_D) &= a_{ji}(\tau, f_D) \cdot u(\tau, f_D) + n_j(\tau, f_D) \end{aligned} \quad (1)$$

The complex weights $a_{ji}(\tau, f_D)$ can then be derived from a cross-correlation of the $u_j(\tau, f_D)$ and $u_i(\tau, f_D)$

$$a_{ji}(\tau, f_D) = \frac{E[u_j(\tau, f_D) \cdot u_i^*(\tau, f_D)]}{E[|u_i(\tau, f_D)|^2] - E[|n_i(\tau, f_D)|^2]} \quad (2)$$

where the expectation $E[\cdot]$ is approximated by averaging over a local neighbourhood \mathcal{N} of the range-Doppler bin (τ, f_D) . To ensure consistency and improve the estimation accuracy, it is suggested to evaluate all feed pairs jointly in a matrix-like approach. The contribution from the noise $n_i(\tau, f_D)$ can either be neglected by restricting the evaluation to samples with very high SNR (i.e. $|u_i| \gg |n_i|$), or be measured separately. The proposed technique is very accurate, as the Tx pattern and scene reflectivity cancel for each range-Doppler bin.

3 Performance Simulation

This section shows an example of how the multichannel radar data acquired in the LPAC mode can be used to improve the elevation beamforming in a reflector SAR system like Tandem-L. For this purpose, we simulate a time series of multichannel radar data, as they would be recorded by a dedicated LPAC data take. To simplify the calculations, we model the backscatter by independent and identically distributed complex Gaussian noise, but a more refined simulation could also use real radar data to better account for inhomogeneities in the backscatter statistics. After range compression and appropriate consideration of the radar imaging geometry⁶, the simulated

⁶ This includes the incorporation of the known scene topography. The simulation in this paper assumes the same geometry and spherical Earth model with flat topography as in [18].

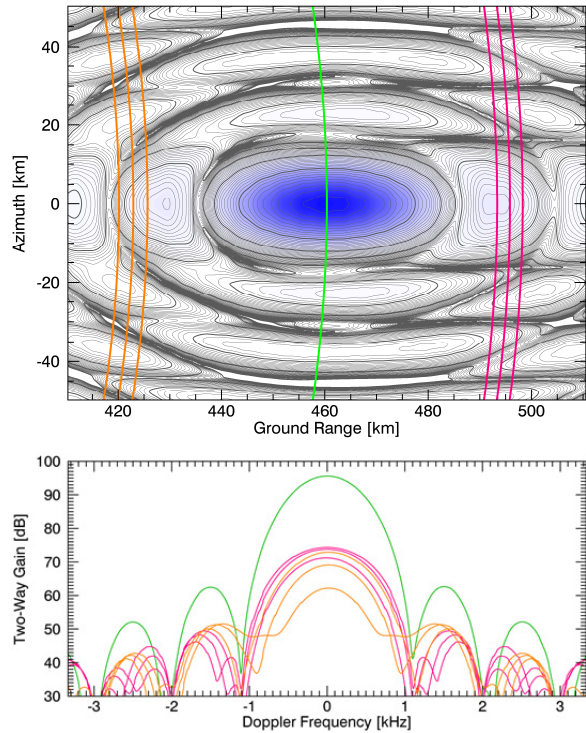


Figure 3: Simulated Tandem-L pattern for an optimum MVDR beamformer that is steered in elevation to a ground range of 460 km assuming full knowledge of each complex feed pattern. The top figure shows the 2-D two-way pattern which is projected on a spherical Earth, while the bottom shows 1-D pattern cuts for fixed range bins corresponding to the swath echo and range ambiguities for PRIs of 130, 140 and 150 μ s. The desired swath echo is shown in green, while the near and far range ambiguities are shown in orange and magenta, respectively.

multichannel radar data are obtained for each radar channel and range line by projecting the antenna-weighted backscatter along iso-range contours (cf. green line in the upper plot of Figure 3, which shows the 2-D antenna pattern of an optimum MVDR beamformer steered towards this range). To provide a realistic weighting, we use here the results from GRASP computations that predict, for each feed element, the two-dimensional complex antenna pattern for the nominal Tandem-L antenna geometry. The computation is then repeated for all transmitted pulses such that we obtain, for each range r , a time series of radar signals $u_i(t_k; r)$, where $i \in \{1, \dots, N_{Rx}\}$ denotes the receive channel (i.e. feed element) and $k \in \{1, \dots, K\}$ the number of the transmitted pulse. To account for thermal noise in each channel, we further add to each of the simulated radar signals white noise, the power of which is calculated from the predicted NESZ in the LPAC mode and the strength of the backscattered signal.⁷

⁷ The simulations in this paper assume equal noise level for all channels where a total SNR of 20 dB would be achieved after applying an optimum MVDR beamformer. The high SNR is not necessary, but nevertheless justified by assuming a backscatter coefficient of -15 dB and an NESZ of -35 dB in the LPAC mode. The low NESZ is due to the reduced bandwidth in the transparency mode.

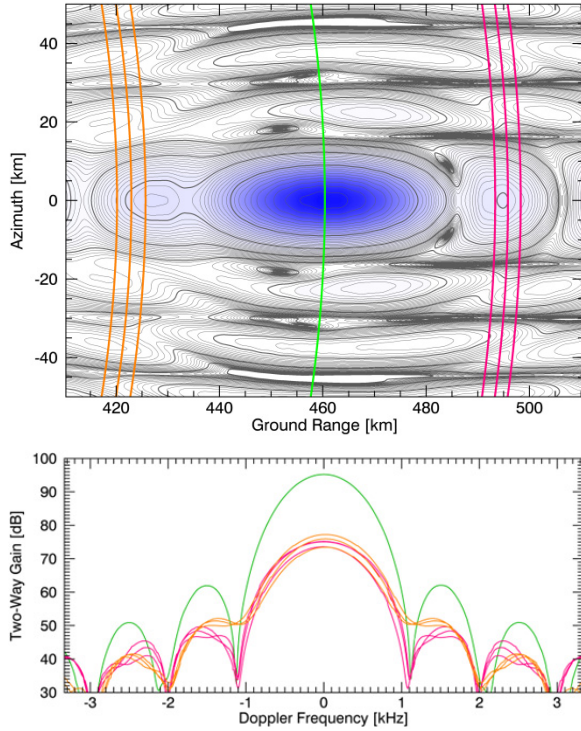


Figure 4: Tandem-L pattern for a beamformer with complex weights provided by the eigenvector decomposition of the covariance matrix. The covariance matrix was estimated from a simulated data acquisition in the LPAC mode. The eigenvector corresponding to the maximum eigenvalue has been used as a weight vector. See Figure 3 for further information.

The N_{Rx} radar signals $u_i(t_k; r)$, which are free of range ambiguities due to the data acquisition in LPAC mode, can then be used to compute, for each range, an estimate of the covariance matrix

$$R_{ij}(r) = E[u_i(t_k; r) u_j^*(t_k; r)] \quad (3)$$

where the expectation operator $E[\cdot]$ is replaced by a sum over the time samples k . From this matrix, we can now derive, again for each range bin r , a weight vector that steers a high gain beam towards the direction of the recorded radar echoes. While there exist several options to exploit the covariance matrix for this purpose, we use here a beamformer where the weights are provided by the conjugate complex of the eigenvector which corresponds to the maximum eigenvalue of the covariance matrix $R_{ij}(r)$. The resulting 2-D antenna pattern and a set of iso-range slices to be explained in the next paragraph are shown in Figure 4. It becomes clear that this eigenvector beamformer has succeeded in steering a highly directive beam towards the desired range using only the simulated radar data acquired in the LPAC mode, but no explicit knowledge of the individual feed patterns. A quantitative comparison with the MVDR beamformer from Figure 3, which maximizes the SNR for a given direction and makes full use of the precise knowledge of all individual feed patterns, reveals moreover that the LPAC eigenvector beamformer has a gain loss of less than 0.4 dB if compared to the optimum MVDR beamformer (see also Figure 6).

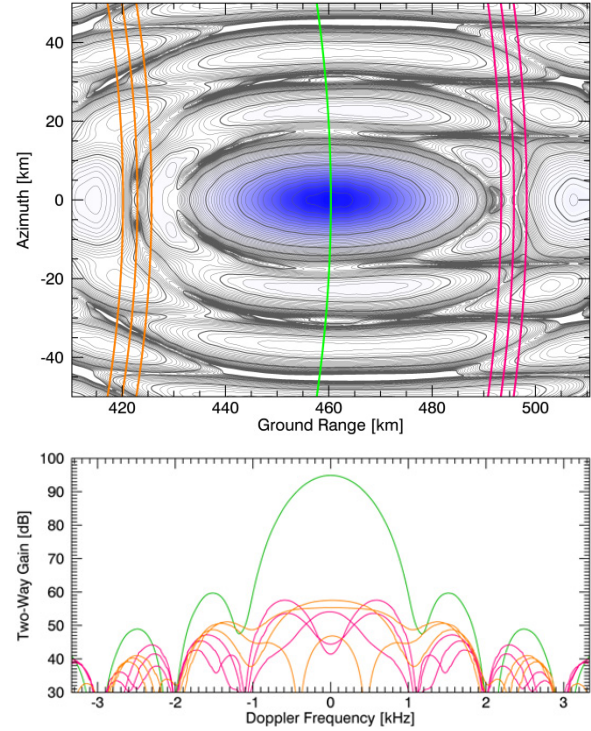


Figure 5: Tandem-L pattern for a beamformer with complex weights provided by a minimum mean square error (MMSE) approach (Wiener beamformer). The desired signal is derived from the unambiguous multichannel radar data acquired in the LPAC mode using the beamformer from Figure 4. The corrupted signal is derived by superimposing the multichannel LPAC data from the unambiguous range with the corresponding data for the range ambiguous positions. A comparison with Figure 3 and Figure 4 reveals that the ambiguity suppression has improved by more than 15 dB.

The eigenvector beamformer can now be used to extract, for each range r , a desired signal $u_d(t_k; r)$ which is free of range ambiguities due to the acquisition in LPAC mode. Furthermore, for each channel a corrupted signal $u_{c,i}(t_k; r)$ contaminated with range ambiguities can be simulated by a linear superposition of the simulated feed signals from different ranges:

$$u_{c,i}(t_k; r) = u_i(t_k; r) + \sum_m a_m u_i(t_k; r - r_m) \quad (4)$$

where r_m denotes the range of ambiguity m . To account for a backscatter difference between the desired and the ambiguous signals, we have moreover introduced a scaling factor a_m .⁸ Based on these data, we may now minimize the mean square error between the desired signal $u_d(t_k; r)$ and a weighted superposition of the corrupted data $u_{c,i}(t_k; r)$. The corresponding beamformer is known as Wiener beamformer, where the weights are derived by multiplying the covariance matrix of the corrupted signals with a vector obtained by correlating the corrupted feed signals with the desired signal. Figure 5 shows the resulting antenna pattern that has been obtained from such a simulation, where three

⁸ A more accurate simulation should include the scaling factor in the backscatter to avoid any scaling of the thermal noise.

near and three far range ambiguities have been simulated and the strength of each ambiguity has been set to $a_m = 1$. A comparison with Figure 3 and Figure 4 reveals that the ambiguity rejection is improved from approximately -20 dB to -37 dB, which reduces the ambiguity power by a factor of more than 40.

4 Discussion

This paper introduced a set of new antenna calibration modes and techniques for multichannel reflector SAR systems. The proposed modes are well suited to acquire information about the relative amplitude and phase of the secondary far-field patterns associated with pairs of feed elements/channels. This mutual pattern information can then be used to improve the performance of advanced real-time beamformers that maximize their gain towards the direction of arrival of the desired radar echo and suppress, at the same time, range ambiguities arriving from different directions. Such beamformers are of great benefit for advanced SAR imaging modes like staggered SAR, which employs multiple elevation beams to map a wide image swath with high resolution.

As the proposed technique does not depend on dedicated calibration targets, it can be used anywhere in the orbit, provided the scene has a known and sufficiently flat topography. To simplify the derivation of optimized beams in the LPAC mode, it is moreover advisable to use a scene with homogeneous and sufficiently strong backscatter as, e.g., provided by rainforests. The 2-D calibration with the HPAC mode may, on the other hand, also benefit from inhomogeneous backscatter to obtain further information about low sidelobes. In this context, permanent scatterers may offer a promising potential for advanced multichannel SAR calibration.

The proposed LPAC mode can not only provide optimized beamforming weights to suppress range ambiguities, but also offers a new opportunity to improve nadir suppression. This prospect is of high interest for advanced imaging modes like staggered SAR, which is susceptible to nadir echoes. To this aim, the LPAC data recording must include the nadir return, which is treated as an additional directional interference. This interference is then added while deriving the beamforming weights, either for all elevation beams, or at least those which may be superimposed by nadir echoes, taking into account variations in satellite height and nadir topography. To improve the strength of the nadir signal, it may even be advantageous to use extra data takes over flat scenes like calm water. The width of the nadir notch can moreover be increased by combining data from multiple LPAC measurements, each acquired with a slightly different roll angle of the satellite.

While this paper focused on multichannel antenna pattern calibration in Tandem-L and its use for advanced range ambiguity suppression, the proposed technique is neither limited to reflector antennas nor to beamforming in elevation. For example, a dedicated data take with a narrow azimuth Tx beam is well suited to derive the relative antenna patterns for a planar HRWS system with multiple azimuth channels.

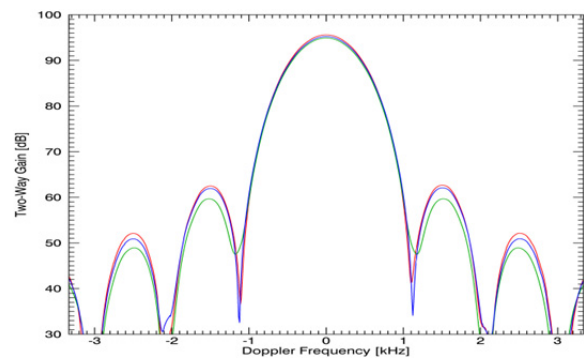


Figure 6: Comparison of the two-way gain for the patterns of Figure 3 (red), Figure 4 (blue) and Figure 5 (green). The two-way patterns are shown for constant reference range as a function of Doppler frequency. The gain loss between the optimum MVDR beamformer, which was derived with full pattern knowledge, and the MMSE beamformer, which was derived from simulated LPAC data and provides enhanced ambiguity suppression, is less than 0.7 dB.

References

- [1] A. Moreira et al., "Tandem-L: A Highly Innovative Bistatic SAR Mission for Global Observation of Dynamic Processes on the Earth's Surface," IEEE Geosci. Remote Sens. Mag., Vol. 3, pp. 8–23, 2015.
- [2] G. Krieger et al., "The Tandem-L Mission Proposal: Monitoring Earth's Dynamics with High Resolution SAR Interferometry," IEEE Radar Conference, Pasadena, USA, 2009.
- [3] S. Huber et al., "Tandem-L: A Technical Perspective on Future Spaceborne SAR Sensors for Earth Observation," in revision.
- [4] S. Huber, M. Younis, A. Patyuchenko, G. Krieger, A. Moreira, "Spaceborne Reflector SAR Systems with Digital Beam-Forming," IEEE Trans. Aerospace Electr. Systems, Vol. 48, pp. 3473–93, 2012.
- [5] J.T. Kare, "Moving Receive Beam Method and Apparatus for Synthetic Aperture Radar," US 6175326 B1, June 29, 1998.
- [6] A. Freeman et al., "SweepSAR: Beam-Forming on Receive using a Reflector-Phased Array Feed Combination for Spaceborne SAR," Proc. IEEE Radar Conference, Pasadena, USA, 2009.
- [7] H. Griffiths, P. Mancini, "Ambiguity Suppression in SARs Using Adaptive Array Techniques," Proc. IGARSS, pp. 1015–18, 1991.
- [8] G. Krieger, N. Gebert, M. Younis, F. Bordoni, A. Patyuchenko, A. Moreira, "Advanced Concepts for Ultra-Wide Swath SAR Imaging," in Proc. EUSAR, Friedrichshafen, Germany, June 2008.
- [9] B. Grafmueller, C. Schaefer, "High resolution synthetic aperture radar device and antenna for one such radar," US 2009/0079621 A1.
- [10] M. Villano, G. Krieger, A. Moreira, "Staggered SAR: High-Resolution Wide-Swath Imaging by Continuous PRI Variation," IEEE Trans. Geosci. Remote Sensing, Vol. 52, pp. 4462–79, 2014.
- [11] M. Villano, G. Krieger, A. Moreira, "A Novel Processing Strategy for Staggered SAR," IEEE Geosci. Remote Sens. Letters, Vol. 11, pp. 1891–95, 2014.
- [12] M. Villano, G. Krieger, A. Moreira, "Staggered SAR: Performance Analysis and Experiments with Real Data," IEEE Trans. Geosci. Remote Sensing, Vol. 55, No. 11, 2017.
- [13] F. Queiroz de Almeida, T. Rommel, M. Younis, G. Krieger, A. Moreira, "Multichannel Staggered SAR: System Concepts with Reflector and Planar Antennas," in revision.
- [14] T. Freeman, "SAR Calibration: An Overview," IEEE Transactions on Geoscience and Remote Sensing, Vol. 30, pp. 1107–1121, 1992.
- [15] J. Reimann, M. Schwerdt, K. Schmidt, N. Tous Ramon, B. Döring, "The DLR Spaceborne SAR Calibration Center," Frequenz, 2017.
- [16] M. Bachmann, M. Schwerdt, B. Bräutigam, "TerraSAR-X Antenna Calibration and Monitoring Based on a Precise Antenna Model," IEEE Trans. Geosci. Remote Sensing, Vol. 48, pp. 690–701, 2010.
- [17] J. Reimann, M. Schwerdt, M. Zink, "Calibration Concepts for Future Low Frequency SAR Missions," CEOS 2016.
- [18] G. Krieger et al., "CEBRAS: Cross Elevation Beam Range Ambiguity Suppression for High-Resolution Wide-Swath and MIMO-SAR Imaging," in Proc. IGARSS, July 2015.